Coordination Geometry

International Edition: DOI: 10.1002/anie.201411959
German Edition: DOI: 10.1002/ange.201411959

Na_4IrO_4: Square-Planar Coordination of a Transition Metal in d^5 Configuration due to Weak On-Site Coulomb Interactions**

*Sudipta Kanungo, Binghai Yan, Patrick Merz, Claudia Felser, and Martin Jansen**

In memory of Rudolf Hoppe

Abstract: *Local environments and valence electron counts primarily determine the electronic states and physical properties of transition-metal complexes. For example, square-planar coordination geometries found in transition-metal oxometalates such as cuprates are usually associated with the d^8 or d^9 electron configuration. In this work, we address an unusual square-planar single oxoanionic $[IrO_4]^{4-}$ species, as observed in Na_4IrO_4 in which Ir^{IV} has a d^5 configuration, and characterize the chemical bonding through experiments and by ab initio calculations. We find that the Ir^{IV} center in ground-state Na_4IrO_4 has square-planar coordination geometry because of the weak Coulomb repulsion of the Ir-5d electrons. In contrast, in its 3d counterpart Na_4CoO_4, the Co^{IV} center is tetrahedrally coordinated because of strong electron correlation. Na_4IrO_4 may thus serve as a simple yet important example to study the ramifications of Hubbard-type Coulomb interactions on local geometries.*

The tetrahedral geometry is by far the most common coordination geometry encountered in isolated $[MO_4]^{n-}$ moieties and is electrostatically favored. Consequently, other coordination geometries, such as square planar, require special local electronic configurations and covalent bonding contributions to be stabilized. It has been quite easy to rationalize the occurrence of square-planar coordination, even in purely qualitative terms, from electron counting. The d^8 and d^9 electronic configurations for transition-metal centers are frequently found to form square-planar complexes,[1] whereas for main group elements, the combination of four covalently bonded ligands and the presence of two lone pairs stringently directs toward the same topology (valence-shell electron-pair repulsion model).[2] Recent work on oxygen-depleted perovskites has somewhat blurred this clear picture. Using soft chemistry routes, a square-planar local geometry has been realized for Fe^{II}, for example, in $SrFeO_2$.[3] However, this compound is reported to be metastable, and its structure does not represent the ground-state configuration. Moreover, the coordination polyhedra are not solitary, but linked via vertices to form 2D sheets. It is thus difficult to judge whether the local geometry is intrinsically stable or rather is supported by extended lattice effects.

The family of $A_4Ir^{IV}O_4$ iridates, synthesized previously with A = Na, K, and Cs[4] by Hoppe and co-workers,[4] featured the first examples of square-planar single oxoanions for a transition-metal center with an alternative electron configuration to d^8 or d^9. As a particularly puzzling fact, Co^{IV} in the lighter homologue Na_4CoO_4 is, as expected, tetrahedrally coordinated in the high-spin d^5 state.[5] Therefore, it is compelling to investigate why Ir^{IV} can be stabilized in the square-planar rather than tetrahedral coordination geometry. Furthermore it would be interesting to determine the factors that induce different local structures for IrO_4 and CoO_4 species in the same oxidation state and to determine whether they can be considered an effect of spin-orbit coupling (SOC), Coulomb interactions, or other effects. Moreover, we are also interested in how these different structures affect the characteristic electronic and magnetic properties of the molecules.

To unravel this apparent conundrum, we revisit this unusual class of square-planar Ir^{IV} iridates by validating earlier structural work, followed by an in depth theoretical analysis of the chemical bonding. Our current study is further motivated by the fact that oxoiridates have attracted much attention in recent years, owing to the interesting emergent phenomena induced by the cooperative effects of Coulomb interactions and SOC, such as spin liquids,[6] topological Mott insulators,[7] and Weyl semi-metals.[8]

All A_4IrO_4 compounds with A = Na, K, and Cs[4] share the same IrO_4 square-planar local environment that determines the electronic and magnetic properties. The Na iridate crystallizes in a tetragonal lattice whereas the K and Cs compounds display lower symmetry monoclinic lattices. For comparison, we chose the highly symmetric Na_4IrO_4 and its 3d analogue Na_4CoO_4 as model systems in this work.

We have prepared Na_4IrO_4 as a pure, single-phase powder, applying the azide/nitrate route.[9] Using Rietveld profile fitting,[10] the earlier crystal-structure determination has been corroborated, confirming the presence of the ideally square-planar IrO_4 moiety. Na_4IrO_4 crystallizes in the tetragonal space group $I4/m$[4] (Figure 1), where the ideal

[*] Prof. Dr. M. Jansen
Max-Planck-Institut für Festkörperforschung
70569 Stuttgart (Germany)
E-mail: m.jansen@fkf.mpg.de
Dr. S. Kanungo, Dr. B. Yan, P. Merz, Prof. Dr. C. Felser, Prof. Dr. M. Jansen
Max-Planck-Institut für Chemische Physik fester Stoffe
01187 Dresden (Germany)
Dr. B. Yan
Max-Planck-Institut für Physik komplexer Systeme
01187 Dresden (Germany)

[**] Acknowledgement is made to the ERC Advanced Grant (291472) and the Deutsche Forschungsgemeinschaft (DFG) through SFB 1143. B.Y. thanks P. Adler for helpful discussions.

Supporting information for this article is available on the WWW under http://dx.doi.org/10.1002/anie.201411959.

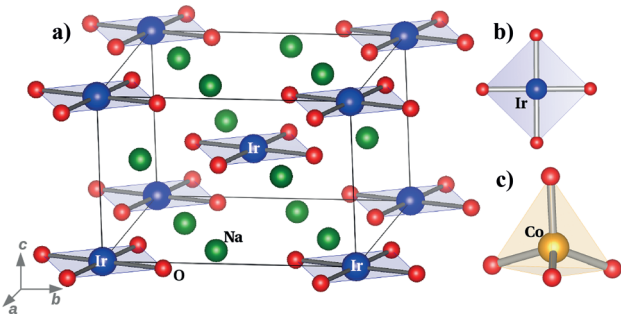

Figure 1. a) X-ray crystal structure of Na_4IrO_4. Atom colors: Na = green, Ir = blue, O = red. b) The square-planar coordination geometry of the IrO_4 species, where the Ir–O bond length is $d_{Ir-O} = 1.902$ Å. (c) The tetrahedral environment of the CoO_4 moiety (orange sphere = Co) in Na_4CoO_4, where the average Co–O bond length is $d_{Co-O} = 1.732$ Å.

square-planar coordination environment of the IrO_4 moiety occurs in the *ab* plane. In contrast, Na_4CoO_4 exhibits a triclinic lattice where the Co center in $[CoO_4]^{4-}$ oxoanion is in a tetrahedral coordination geometry,[5] as shown in Figure 1 c.

The temperature dependence of the magnetic susceptibility (χ) exhibits clear antiferromagnetic ordering for Na_4IrO_4 at low temperature. As shown in Figure 2, the

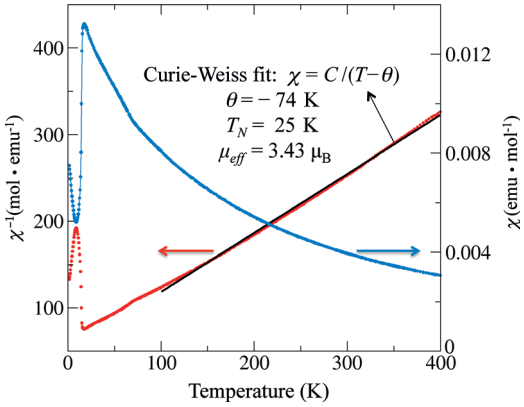

Figure 2. Temperature dependence of the magnetic susceptibility of Na_4IrO_4 measured at a field strength of 3.5 T. The red and blue dots represent χ^{-1} and χ values. The black line is the fitting of χ^{-1} to the temperature according to the Curie–Weiss law in the temperature range of 100–400 K.

antiferromagnetic transition occurred at the Neel temperature ($T_N \approx 25$ K). The inverse of the susceptibility (χ^{-1}) deviated slightly from linearity in the low-temperature region. This is plausibly related to the population of multiplet states, which is beyond the scope of the current work. Fitting the inverse susceptibility in the high-temperature region ($100 < T < 400$ K) according to the Curie–Weiss law, given by $\chi = C/(T-\theta)$, where C and θ are the Curie and Weiss constants, respectively, we obtained $\theta = -74$ K, $C = 1.47$ emu K mol^{-1}, and a μ_{eff} value of 3.43 μ_B (where $\mu_{eff} = 2.83\sqrt{C}$). The determined effective magnetic moment is similar to the ideal magnetic moment of the $S = 3/2$ spin state $\mu_{eff} = 2\sqrt{S(S+1)} =$ 3.87 μ_B, as confirmed in the following theoretical ab initio investigation.

The electronic and magnetic properties were further investigated using DFT calculations within the framework of the generalized gradient approximation (GGA).[11] The correlation effect was included in the GGA + U[12] scheme for transition-metal elements. In the GGA calculations, the lattice parameters and atomic positions of Na_4IrO_4 and Na_4CoO_4 were first fully relaxed. The resultant optimized structures correlated well with experimental values (see the Table S2 in the Supporting Information).[10] When we included the Coulomb on-site interaction U and applied it to Ir-5d and Co-3d states, the ground-state structures remained unchanged for both compounds. For example, the square-planar configuration remained as the ground state of Na_4IrO_4 even up to an unusually large value, $U_{Ir} = 6$ eV.[13] Additionally, a tetrahedral $[IrO_4]^{4-}$ oxoanion exists in a metastable phase only at a very large U_{Ir} value (e.g. 6 eV). If we decreased the U_{Ir} value to smaller than 4 eV, this tetrahedral oxoanion collapsed quickly to form the square-planar analogue in the structure optimization. This lattice instability indicated the significance of effective Coulomb interactions in determining the structure of Na_4IrO_4.

The d orbital splitting under the crystal field (CF) and with corresponding electron occupation of orbitals were extracted from calculations and are shown in Figure 3. In

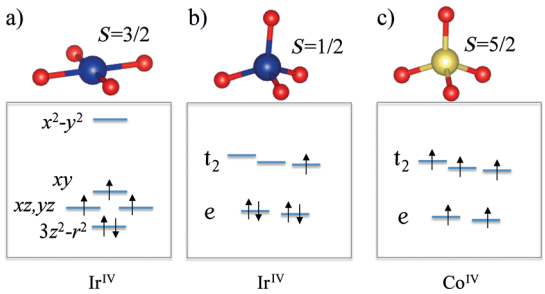

Figure 3. Crystal-field splitting of d orbitals and corresponding orbital occupation for a) the square-planar IrO_4 moiety, b) the tetrahedral IrO_4 group in the artificially fixed tetrahedral Na_4IrO_4 structure, and c) the tetrahedral CoO_4 species.

the square-planar environment of the IrO_4 moiety, Ir (d^5) exhibits an $S = 3/2$ spin state, whereas in the Co^{IV} tetrahedral environment in the CoO_4 moiety, the Co center (d^5) displays an $S = 5/2$ spin state. Both cases opened moderate energy gaps at the Fermi energy. However, when trapping Ir (d^5) in the metastable structure in the tetrahedral crystal field, an orbital filling of $e^4t_2^1$ occurred because of the weak Coulomb U value of Ir-5d states. Consequently, considerable density of states (DOS) appeared at the Fermi energy (Figure 4 b), leading to a Jahn–Teller type instability. Therefore, differences in the structural coordination of $[IrO_4]^{4-}$ and $[CoO_4]^{4-}$ oxoanions can be rationalized by differences in the on-site Coulomb interactions within Ir-5d and Co-3d states.

As shown in Figure 4 a, an energy gap of 0.5 eV between spin-up d_{xy} and spin-down $d_{xz,yz}$ was observed for Na_4IrO_4. From the DOS, we were able to estimate the CF splitting of the square-planar environment of Ir-5d states (Figure 3),

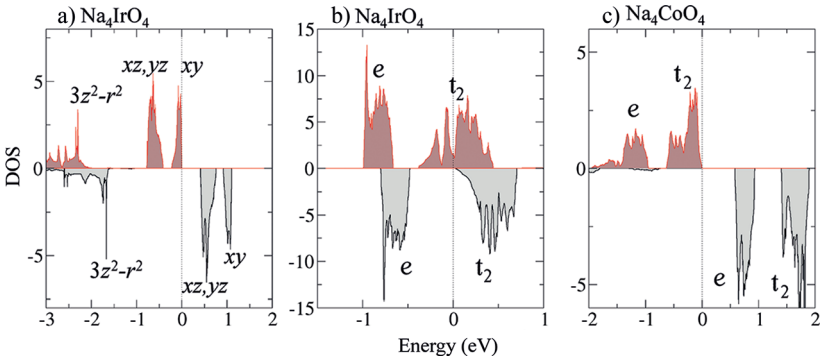

Figure 4. Density of states for a) square-planar Na_4IrO_4, b) tetrahedral Na_4IrO_4, and c) tetrahedral Na_4CoO_4 calculated within the GGA approximation. The Fermi energy is shifted to zero. Positive (red curves) and negative (black curves) values represent spin-up and spin-down channels, respectively.

which accommodates five d electrons. According to Hund's rule, the first four d electrons fill the lowest four levels in the spin-up channel. However, the fifth electron cannot fill the $d_{x^2-y^2}$ level (not shown in Figure 4a) owing to the large CF energy gap ($\approx$4 eV) between d_{xy} and $d_{x^2-y^2}$. It occupies the $d_{3z^2-r^2}$ state in the spin-down mode at the expense of the electron-pairing energy of 1 eV, which is estimated from the energy splitting between spin-down and spin-up $d_{3z^2-r^2}$ levels. Thus, a final $S=3/2$ state is realized, explaining the experimentally observed magnetic moment. In the above calculations, we presumed that the lattice had ferromagnetic order. We also performed calculations with the antiferromagnetic spin configuration, in which spins at the body center and corner sites were oppositely orientated. The antiferromagnetic phase was found to be 25 meV per formula unit lower in energy than the ferromagnetic phase. However, antiferromagnetic and ferromagnetic configurations exhibited the same pattern of CF splitting and orbital filling without any qualitative differences. For the sake of simplicity, we used the ferromagnetic configuration for all further calculations presented in this work. Additionally, the main effect of SOC was to lift the degeneracy of the $d_{xz,yz}$ bands but it did not affect the main features of the orbital diagram or the structure instability. Therefore, we have omitted SOC in the following discussions (see more details on SOC in the Supporting Information).[10]

When $U_{Ir}<4$ eV was applied in GGA + U calculations, which is a reasonable small U value for Ir-5d states, the square-planar structure remains as the ground-state phase, as discussed above. Surprisingly, when a large U_{Ir} value (e.g. 6 eV) is employed, a metastable structure with a tetrahedral IrO_4 moiety was obtained. This tetrahedral environment exhibits e–t_2-type CF levels, which are filled as $e^2t_2^3$ as a result of the artificially large U_{Ir} value. However, if we apply $U_{Ir}<$ 4 eV to this metastable tetrahedral structure, the same CF levels can only be filled as $e^4t_2^1$ (Figure 3b). Then these partially filled t_2 bands induce considerable DOS at the Fermi energy (Figure 4b), although the degeneracy of the t_2 states split slightly because of four non-equivalent Ir–O bonds in the tetrahedral structure. Consequently, a Jahn–Teller type instability emerges and causes the IrO_4 moiety to become square-planar, resulting in an energy gap. Therefore, the relative weak U_{Ir} value was the principal origin of the instability in the tetrahedral structure of the $[IrO_4]^{4-}$ oxoanion.

For Na_4CoO_4, the CF levels are occupied as $e^2t_2^3$ with the $S=5/2$ high-spin state, owing to the large Coulomb U value of Co-3d states. In the GGA calculation, this already leads to an energy gap (Figure 4c). At a large U_{Co} value (e.g. 5 eV) in GGA + U calculations, a value known to be a good approximation for Co, the above scenario still holds. Additionally, we note that the square-planar structure is a metastable phase for Na_4CoO_4, which was found to be energetically 0.4 eV per formula unit higher than the tetrahedral structure in the GGA calculations. Following the trend from 3d to 5d systems, we would expect that the corresponding 4d material Na_4RhO_4 possibly presents an intermediate state between Na_4CoO_4 and Na_4IrO_4, although Na_4RhO_4 has yet to be synthesized experimentally. GGA calculations reveal that Na_4RhO_4 exhibits a distorted tetrahedral environment within the RhO_4 moiety with an $S=1/2$ spin state. Even though partially filled t_2 states appear at the Fermi energy, which is similar to Na_4IrO_4, a slight distortion of the RhO_4 tetrahedra is enough to open an energy gap of 0.1 eV (GGA). This effect is caused by the narrow bandwidth of Rh-t_2 states, whereas the bandwidth of Ir-t_2 states is too wide to open an energy gap. So Na_4RhO_4 can be stabilized at the $S=1/2$ state whereas Na_4IrO_4 cannot (see the Supporting Information).[10] Altogether, the Ir, Rh, and Co compounds constitute an interesting phase diagram, wherein the electron-correlation effect interplays with the crystal structure and magnetic properties. It is possible that materials at critical points between different phases may be synthesized from solid solutions of the two end members Na_4RhO_4 and Na_4IrO_4, for example as $Na_4Rh_xIr_{1-x}O_4$. Such materials may promise unusual characteristics, such as magnetoelastic coupling and electron-lattice coupling.

In summary, we have experimentally confirmed individual oxoanions $[IrO_4]^{4-}$ with ideal square-planar geometry to be constitutive components of the ground-state structure of Na_4IrO_4. We have rationalized this unprecedented local coordination of a transition metal with a d^5 electronic configuration by quantum chemical calculations on the GGA + U level. These calculations showed that weak interatomic Coulomb repulsion is the pivotal force that influences the stabilization of the square-planar coordination of a central cation in the $5d^5$ electronic configuration. As a result of the weak U value of Ir-5d electrons, the square-planar coordination geometry is the most favorable one for $[IrO_4]^{4-}$. In contrast, as a result of the strong U value of Co-3d states, the $[CoO_4]^{4-}$ oxoanion, for example, in Na_4CoO_4, adopts the tetrahedral geometry associated with a high-spin $S=5/2$ state. These findings introduce the strength of Coulomb repulsion, commonly expressed as the Hubbard U parameter, as another independent parameter to explain electronically driven distortions of local topologies, in addition to the Jahn–Teller effect and spin-orbit coupling.[15]

Experimental Section

For the preparation of Na_4IrO_4, sodium azide (Alfa Aesar, 99%), sodium nitrate (Merck, 99.99%), and iridium oxide IrO_2 were employed. IrO_2 was obtained after heating $IrCl_3{\cdot}xH_2O$ (Alfa Aesar, 99.9%) at 650 °C for 24 h under an oxygen flow. The starting materials were mixed according to the following equation, using a 2.5% excess of the sodium compounds: $10\,NaN_3 + 2\,NaNO_3 + 3\,IrO_2 \rightarrow 3\,Na4\,IrO_4 + 16\,N_2$. The compounds were mixed in an agate mortar into a fine powder and pressed into pellets (ø 13 mm, 5×10^4 N, 5 min). After drying overnight under vacuum (10^{-3} mbar) at 120 °C, the pellets were placed under argon in a special steel vessel equipped with a silver inlay.[9] Under a slow argon flow, the following temperature treatment was applied: 25 °C→250 °C (100 °C h^{-1}), 250 °C→380 °C (5 °C h^{-1}), 380 °C→600 °C (20 °C h^{-1}), and subsequent annealing for 50 h at 600 °C before cooling down to room temperature at a rate of −20 °C h^{-1}. The as-obtained black microcrystalline powder appeared red after further cleaving under dried kerosene, and decomposed in water forming a dark-blue solution. As the samples were sensitive to humid air, they were sealed in glass ampoules under argon and all manipulations were performed under a strict inert atmosphere of purified argon. Laboratory X-ray powder diffraction (XRPD) studies were performed with an X'Pert PRO diffractometer (PANalytical B.V., Netherlands) employing Cu-$K\alpha$1 radiation (λ = 0.154056 nm). XPRD was recorded at room temperature in a 2θ range 10–120°. The magnetization was measured in the temperature range from 0.8 to 400 K using a Quantum design MPMS-XL7 SQUID magnetometer.

Theoretical calculations: DFT calculations were performed within the plane-wave basis set based on pseudopotentials as implemented in the Vienna ab initio simulation package (VASP).[14] The Perdew–Burke–Ernzerhof type GGA functional was employed.[11] The on-site electron–electron repulsion beyond the GGA was taken into account through GGA + U[12] calculations. For the plane-wave basis, a 500 eV plane-wave cutoff was applied. A k-point mesh of $8\times8\times6$ in the Brillouin zone was used for self-consistent calculations. In the structural optimization, both the atomic positions and the lattice parameters were fully optimized without constrains. The positions of the atoms were relaxed toward equilibrium until the force became less than 0.01 eV $Å^{-1}$. Hybrid-functional calculations were also employed to validate the GGA + U results.[10]

Keywords: ab initio calculations · coordination geometry · electronic structure · oxometalates · transition metals

How to cite: *Angew. Chem. Int. Ed.* **2015**, *54*, 5417–5420
Angew. Chem. **2015**, *127*, 5507–5510

[1] A. F. Holleman, E. Wiberg, *Lehrbuch der Anorganischen Chemie*, 102nd ed., Walter de Gruyter, Berlin, **2007**.
[2] R. J. Gillespie, E. A. Robinson, *Angew. Chem. Int. Ed. Engl.* **1996**, *35*, 495; *Angew. Chem.* **1996**, *108*, 539.
[3] Y. Tsujimoto, C. Tassel, N. Hayashi, T. Watanabe, H. Kageyama, K. Yoshimura, M. Takano, M. Ceretti, C. Ritter, W. Paulus, *Nature* **2007**, *450*, 1062.
[4] a) P. Kroeschell, R. Hoppe, *Naturwiss.* **1985**, *72*, 442; b) K. Mader, R. Hoppe, *Z. Anorg. Allg. Chem.* **1992**, *614*, 30; c) K. Mader, R. Hoppe, *Z. Anorg. Allg. Chem.* **1993**, *619*, 1647.
[5] a) M. Jansen, *Z. Anorg. Allg. Chem.* **1975**, *417*, 35; b) C. Jeannot, B. Malaman, R. Gérardin, B. Oulladiaf, *J. Solid State Chem.* **2002**, *165*, 266.
[6] a) P. W. Anderson, *Mater. Res. Bull.* **1973**, *8*, 153; b) Y. Okamoto, M. Nohara, H. Aruga-Katori, H. Takagi, *Phys. Rev. Lett.* **2007**, *99*, 137207.
[7] a) D. Pesin, L. Balents, *Nature Phys.* **2010**, *6*, 376; b) B.-J. Yang, Y. B. Kim, *Phys. Rev. B* **2010**, *82*, 085111.
[8] X. Wan, A. M. Turner, A. Vishwanath, S. Y. Savrasov, *Phys. Rev. B* **2011**, *83*, 205101.
[9] M. Jansen, *Z. Anorg. Allg. Chem.* **2012**, *638*, 1910.
[10] See the Supporting Information for experimental and calculation details.
[11] J. P. Perdew, K. Burke, M. Ernzerhof, *Phys. Rev. Lett.* **1996**, *77*, 3865.
[12] a) V. I. Anisimov, J. Zaanen, O. K. Andersen, *Phys. Rev. B* **1991**, *44*, 943; b) V. I. Anisimov, A. I. Poteryaev, M. A. Korotin, A. O. Anokhin, G. Kotliar, *J. Phys. Condens. Matter* **1997**, *9*, 7359; c) S. L. Dudarev, S. Y. Savrasov, C. J. Humphreys, A. P. Sutton, *Phys. Rev. B* **1998**, *57*, 1505.
[13] I. V. Solovyev, P. H. Dederichs, *Phys. Rev. B* **1994**, *50*, 16861.
[14] a) G. Kresse, J. Hafner, *Phys. Rev. B* **1993**, *47*, 558; b) G. Kresse, J. Furthmüller, *Phys. Rev. B* **1996**, *54*, 11169.
[15] F. Wang, U. Wedig, D. L. V. K. Prasad, M. Jansen, *J. Am. Chem. Soc.* **2012**, *134*, 19884.

Received: December 16, 2014
Revised: February 6, 2015
Published online: March 13, 2015

